Chromatin condensation modulates access and binding of nuclear proteins

Robert M. Martin[1] and M.Cristina Cardoso[1,2*]

[1] Max Delbrück Center for Molecular Medicine, 13125 Berlin, Germany

[2] Darmstadt University of Technology, Department of Biology, 64287 Darmstadt, Germany

* Correspondence to: M. Cristina Cardoso, e-mail: cardoso@mdc-berlin.de, Tel. +49-30-94062109, Fax +49-30-94063343

Running title

Dynamics of chromatin accessibility

Abstract

The condensation level of chromatin is controlled by epigenetic modifications and associated regulatory factors that change throughout differentiation and cell cycle progression. To test whether changes of chromatin condensation levels *per se* affect access and binding of proteins we used a hypertonic cell treatment. This shift to hyperosmolar media caused increased nuclear calcium concentrations and induced a reversible chromatin condensation comparable to levels in mitosis but independent of mitotic histone H3 serine 10 phosphorylation. Photobleaching experiments with H2B-GFP and GFP-HP1α before and after induced chromatin condensation showed that the exchange of integral as well as associated chromatin proteins is affected. Photoactivation of PAGFP-HP1α demonstrated that hypercondensation reduces the dissociation rate and stabilized HP1 chromatin binding. Finally, measuring the distribution of nucleoplasmic proteins in the range from 30 to 230 kDa we found that even relatively small proteins like GFP are at least partially excluded from hypercondensed chromatin in living cells. These results suggest that structural changes in condensed chromatin by themselves affect chromatin access and binding of chromatin proteins independent of regulatory histone modifications.

Key words

Chromatin accessibility, chromatin condensation, fluorescence microscopy, photoactivation, photobleaching

The cell nucleus is a highly organized organelle storing and translating genetic information. Although there are no substructures separated by membranes, the nucleus is compartmentalized for different functions in nucleic acid metabolism.[1] The nuclear DNA is organized together with structural proteins into dynamic higher order chromatin structures, which reflect and control gene expression during the cell cycle and cellular differentiation.[2,3] As a consequence of a complex and not yet understood interplay between chromatin condensation state, transcriptional activity and modifications of chromatin organizing proteins, chromatin subsets are termed eu- and heterochromatin.[4,5] Euchromatin in interphase cells is actively transcribed and less condensed while heterochromatin is transcriptionally inactive with a condensation level similar to mitotic chromosomes.[6] During mitotic chromatin condensation, DNA metabolism (e.g., transcription and replication) stops and only resumes after chromatin decondensation in early G1 phase. The condensation of chromatin is characterized by a reduction of volume due to a spatial organization into densely packed higher order structures.[7] Specific histone modifications, e.g. histone H1 and H3 phosphorylation, occur at mitosis and contribute to the individualization and condensation of chromosomes. The consequences of this compaction into condensed chromosomes at mitosis are reduced free volumes and less exposed surface of the chromatin substructures on which molecules could interact.[8,9] However, it is unclear whether and how changes in the chromatin condensation state and/or histone modifications affect the distribution and access of nucleoplasmic proteins and the mobility of chromatin organizing proteins.

Interphase chromatin has been shown to be accessible to macromolecules[10,11], chromatin proteins[12] and neutral inert proteins even at the single molecule level [13]. Furthermore, certain transcription and chromatin factors have been shown to still have access to chromosomes in mitosis when the DNA metabolism stops.[14] Therefore, the relationship between nuclear protein distribution, chromatin accessibility and how changes in chromatin condensation over the cell cycle impact on DNA metabolism remains unclear. In this study, we have manipulated chromatin condensation in interphase cells to test whether the level of chromatin condensation independently of mitotic histone modifications can impact on mobility and accessibility of nuclear proteins.

Manipulation and quantitative evaluation of chromatin condensation mechanisms

The maximal chromatin condensation takes place at every mitosis in cycling cells and results in a cessation of DNA metabolism. The latter could be the result of M-phase specific modifications of chromatin proteins (e.g., histone modifications) directly preventing the access of factors to the genome and/or structural changes of chromatin hindering access by increased compaction. To distinguish between these possibilities, we made use of an approach to induce hypercondensation of chromatin during interphase.[15]

We first compared the chromatin volumes of individual living HeLa cells labeled with histone H2B-GFP fusion proteins in different cell cycle stages and after chromatin condensing treatment. The same cells were imaged beginning in mitosis and through reentry into G1 followed by induced chromatin condensation by incubation in hyperosmolar medium for 5 minutes. We then measured the chromatin volumes in the three conditions to test whether the treatment reduced interphase chromatin volumes to the level of mitotic chromosome volumes (Fig 1). The chromatin volume measurements for mitosis and hyperosmolar condensation in G1 showed similar levels of 39% ± sd 9% and 40% ± sd 11% respectively, relative to G1 chromatin in the same cells before treatment (Fig 1). This hypercondensation of chromatin was reversible within 10 minutes of returning to normal osmolar medium and resulting in cessation of DNA metabolic processes such as transcription and replication (data not show and [15]). We, therefore, conclude that this approach generated condensation of chromatin in interphase nuclei to the same extent as mitotic chromatin.

Next, we assessed the occurrence of typical chromatin modifications in mitotic chromosomes and hypercondensed interphase chromatin. At mitosis, phosphorylated histone H3 at serine 10 is associated with the individualization and condensation of chromosomes.[16] Although we found similar levels of chromatin condensation (Fig 1), no mitosis specific histone H3 phosphorylation was detected (Fig 2A). Hence, the process of hyperosmolar chromatin condensation relies on a different pathway, which does not involve cell cycle specific histone modifications but rather profound structural changes.

Since we had previously reported that cellular energy depletion using Na-azide leads to interphase chromatin condensation with increased calcium level in the nucleus[17], we measured the levels of this cation using the fluorescent calcium sensor Fluo 3 before and after hypertonic treatment. Our data demonstrates that the condensation of chromatin by hyperosmolarity is accompanied by a

seven-fold rise in the intranuclear calcium level (Fig 2B). Subsequent addition of the calcium ionophore ionomycin to the cells led to an even higher increase establishing that our measurements were not performed under saturating conditions.

Taken together these results indicate that reversible hypercondensation of interphase chromatin occurs in the absence of mitotic histone modifications, likely as a result of increased intranuclear calcium levels, and leads to a stop in DNA metabolism.

Accessibility of proteins to different chromatin condensation states

Next, we assayed the impact of chromatin condensation levels on the accessibility of nuclear proteins.

Large number of nuclear proteins bind to or are incorporated into chromatin structures throughout the cell cycle. We therefore tested whether chromatin condensation level affects their access to and their dynamics at chromatin. We selected a nucleosome core histone (H2B) and a heterochromatin binding protein (HP1) as representative chromatin proteins and analyzed their chromatin access and mobility by photobleaching and photoactivation experiments.

The nucleosome protein H2B-GFP was not redistributed upon hyperosmotic chromatin hypercondensation (Fig 3A). Fluorescence recovery after photobleaching (FRAP) analysis showed, in accordance to previous reports[12], that the half-time of recovery ($t_{1/2}$) in interphase chromatin for this core histone was about 180 min. Upon hyperosmolar treatment, only about 5% fluorescence recovery could be measured within the same time, indicating that the access to and/ or release of the core histone H2B from fully condensed interphase chromatin was affected.

Chromatin proteins that are not core components of the nucleosome often associate less tightly to chromatin and DNA than histones. The heterochromatin protein HP1α binds to methylated histone H3 and accumulates in heterochromatin. We measured the half recovery time of GFP-HP1α in interphase heterochromatin of HeLa cells and compared it with hypercondensed chromatin in interphase and mitotic cells. In interphase heterochromatin the $t_{1/2}$ was 2 s (Fig 3B), which fits well with previously reported half recovery times of 1 to 10 s.[18,19] In hypercondensed interphase chromatin though HP1α recovery in the FRAP analysis was slower with a $t_{1/2}$ increased to 20 s. To clarify whether HP1α was transiently trapped in the hypercondensed interphase chromatin, we performed photoactivation experiments and measured the dissociation of fluorescent PAGFP-

HP1α molecules from the heterochromatin spots in the photoactivated area. Analysis of the fluorescence decay curves (Fig 3C) revealed that HP1α $t_{1/2}$ of dissociation from interphase heterochromatin was 8 s, compared to a 6.5 fold slower $t_{1/2}$ of 52 s in hypercondensed interphase chromatin. These results indicate a reduced mobility and a transient trapping of HP1α.

Taken together we could demonstrate that the hypercondensed interphase chromatin was less accessible and reduced the exchange of chromatin proteins like core histones and heterochromatin binding proteins.

We then measured the access of non-chromatin proteins to the differently condensed chromatin. We chose GFP as a neutral probe protein and imaged the same cells before and after hyperosmolar treatment to directly compare the distribution of proteins relative to chromatin within the same cell. Furthermore, we compared the results to mitotic chromatin.

Fig 4 shows confocal optical sections of living cells displaying the distribution of the inert tracer protein GFP relative to H2B-mRFP labeled chromatin. The relative distribution was then analyzed quantitatively first by plotting the GFP signal intensity versus the histone-labeled chromatin along a line across the nucleus (linescan analysis, Fig 4B) and second by a correlation analysis (Fig 4C). The latter included both the display of all red and green pixels within the nucleus, excluding the nucleoli, in intensity scatter plots, and the calculation of the Pearson's coefficient R as a measure for correlation (+1), anti-correlation (-1) or no correlation (0) of two color channels in images.[20]

In mitosis the GFP was mostly excluded from chromatin, visible as dark areas where the chromosomes are located (Fig 4A, left column). The exclusion is displayed in the linescan by a drop of the GFP intensity and inverse progression of the chromatin intensity. The scatter plot showed a distribution in a sharp cone of moderate negative slope, with the lowest GFP intensities in the region of occupied by the chromosomes. Finally, the Pearson's correlation coefficient of R = -0.8 ± sd 0.2 clearly demonstrated an anti-correlation of GFP and mitotic chromosomes. In the interphase cell (Fig 4A, middle column) GFP showed an overall much more homogeneous distribution throughout the nucleus with exception of the nucleoli, corroborated further by the linescan analysis depicting a reduction of GFP in the nucleoli (Fig 4B, arrowhead). In some larger heterochromatin spots we could observe some reduction of the GFP concentration (Fig 4B, arrow). The scatter plot displayed the GFP and chromatin pixel intensities as a cloud in the center of the plot and the R-value of -0.1 ± sd 0.1 close to zero indicated no correlation (Fig 4C). After induced

condensation of interphase chromatin to mitotic chromosome volume, a chromatin network like structure became apparent. The GFP redistributed mostly to the regions not occupied by chromatin, which corresponded to an enlarged interchromatin space (Fig 4A, right column). The GFP exclusion from condensed interphase chromatin was clearly shown by the inverse correlation of the linescan data (Fig 4B) and the shift towards a negative slope on the scatter plot and the negative R-value of -0.6 ± sd 0.1 (Fig 4C).

To test whether this exclusion of proteins from the compacted chromatin was a general phenomenon for non chromatin bound nuclear proteins we extended this analysis to several nucleoplasmic proteins of increasing size up to 230 kDa (Fig S1). As for GFP, all proteins tested independent of their size showed a similar level negative correlation with mitotic as well as interphase hypercondensed chromatin.

In summary, making use of a hypertonic treatment we could achieve in interphase cells a chromatin condensation level similar to mitotic chromosomes in the absence of the typical mitotic histone modifications and likely due to increased intranuclear calcium level. Increasing the chromatin condensation lead to a slowed exchange of chromatin proteins. Furthermore, although in general interphase chromatin was accessible to non-chromatin proteins within a size range of 30-230 kDa, upon hypercondensation they redistributed away and exhibited an anti-correlated distribution to the same level than to mitotic chromatin. This concentration reduction of non chromatin proteins could therefore, concomitantly with other chromatin modifications, be involved in the shutdown of DNA metabolism in mitosis. These data are also consistent with the results from our recent analysis of the mobility and access of single streptavidin proteins to heterochromatin where these interphase chromatin domains exhibited quite some permeability to this neutral average sized protein.[13]

It has been debated over the past years whether and how chromatin can exclude nuclear factors and the contribution of this effect for DNA metabolism and heterochromatin function. Different studies indicated that macromolecules have access to interphase chromatin. However, these studies have used carbohydrates like dextrans, which may behave differently from nuclear proteins.[21,10] In addition, access to chromatin was not analyzed at different condensation levels. Photodynamic studies showed that chromatin in interphase and mitosis is accessible to chromatin factors like histones and heterochromatin proteins.[14,22,19] Our data also showed that condensed

chromatin was accessible to nucleosomal proteins and other chromatin associated factors that are involved in heterochromatin maintenance. On the other hand, our results indicate that the concentration of nucleoplasmic proteins that are not associated with nucleosomes is low in chromatin with higher condensation level. We suggest that the partial exclusion of nucleoplasmic proteins is due to increased structural restrictions and dense environments occupied by condensed chromatin and concentrated chromatin binding factors. In the condensed chromatin structures the competition for available volume favors high affinity chromatin binding factors and decreases the number of nucleoplasmic proteins with less or no affinity to those structures. In mitosis the reduced access of proteins could, in addition to specific chromatin modifications, reduce genome wide accessibility and, thereby, contribute to the mitotic shutdown of transcription, replication and other DNA dependent processes. The modulation of protein access and consequently local protein concentration could constitute a general mechanism for the regulation of binding dynamics, enzymatic activities and DNA metabolism.

Acknowledgements

We thank Sabine Görisch for many discussions, Jeffrey H. Stear for comments on the manuscript and Ulrike Ziebold for the kind gift of anti-phospho H3 antibody. We are indebted to Heinrich Leonhardt for numerous discussions and helpful suggestions throughout the course of this project. This work was funded by grants of the German Research Council (DFG) to MCC.

References

1. Cremer, T., Kreth, G., Koester, H., Fink, R. H., Heintzmann, R., Cremer, M., Solovei, I., Zink, D. & Cremer, C. (2000). Chromosome territories, interchromatin domain compartment, and nuclear matrix: an integrated view of the functional nuclear architecture. *Crit Rev Eukaryot Gene Expr* **10**, 179-212.
2. Belmont, A. S., Dietzel, S., Nye, A. C., Strukov, Y. G. & Tumbar, T. (1999). Large-scale chromatin structure and function. *Curr Opin Cell Biol* **11**, 307-11.
3. Cremer, T., Kupper, K., Dietzel, S. & Fakan, S. (2004). Higher order chromatin architecture in the cell nucleus: on the way from structure to function. *Biol Cell* **96**, 555-67.
4. Richards, E. J. & Elgin, S. C. (2002). Epigenetic codes for heterochromatin formation and silencing: rounding up the usual suspects. *Cell* **108**, 489-500.
5. Kouzarides, T. (2007). Chromatin modifications and their function. *Cell* **128**, 693-705.
6. Francastel, C., Schubeler, D., Martin, D. I. & Groudine, M. (2000). Nuclear compartmentalization and gene activity. *Nat Rev Mol Cell Biol* **1**, 137-43.
7. Mora-Bermudez, F. & Ellenberg, J. (2007). Measuring structural dynamics of chromosomes in living cells by fluorescence microscopy. *Methods* **41**, 158-67.
8. Belmont, A. S. (2006). Mitotic chromosome structure and condensation. *Curr Opin Cell Biol* **18**, 632-8.
9. Daban, J. R. (2003). High concentration of DNA in condensed chromatin. *Biochem Cell Biol* **81**, 91-9.
10. Verschure, P. J., Van Der Kraan, I., Manders, E. M., Hoogstraten, D., Houtsmuller, A. B. & Van Driel, R. (2003). Condensed chromatin domains in the mammalian nucleus are accessible to large macromolecules. *EMBO Rep* **4**, 861-866.
11. Görisch, S. M., Wachsmuth, M., Toth, K. F., Lichter, P. & Rippe, K. (2005). Histone acetylation increases chromatin accessibility. *J Cell Sci* **118**, 5825-34.
12. Kimura, H. & Cook, P. R. (2001). Kinetics of core histones in living human cells: little exchange of H3 and H4 and some rapid exchange of H2B. *J Cell Biol* **153**, 1341-53.
13. Grünwald, D., Martin, R. M., Buschmann, V., Bazett-Jones, D. P., Leonhardt, H., Kubitscheck, U. & Cardoso, M. C. (2008). Probing intranuclear environments at the single-molecule level. *Biophys J* **94**, 2847-58.

14. Chen, D., Dundr, M., Wang, C., Leung, A., Lamond, A., Misteli, T. & Huang, S. (2005). Condensed mitotic chromatin is accessible to transcription factors and chromatin structural proteins. *J Cell Biol* **168**, 41-54.

15. Albiez, H., Cremer, M., Tiberi, C., Vecchio, L., Schermelleh, L., Dittrich, S., Kupper, K., Joffe, B., Thormeyer, T., von Hase, J., Yang, S., Rohr, K., Leonhardt, H., Solovei, I., Cremer, C., Fakan, S. & Cremer, T. (2006). Chromatin domains and the interchromatin compartment form structurally defined and functionally interacting nuclear networks. *Chromosome Res* **14**, 707-33.

16. Hendzel, M. J., Wei, Y., Mancini, M. A., Van Hooser, A., Ranalli, T., Brinkley, B. R., Bazett-Jones, D. P. & Allis, C. D. (1997). Mitosis-specific phosphorylation of histone H3 initiates primarily within pericentromeric heterochromatin during G2 and spreads in an ordered fashion coincident with mitotic chromosome condensation. *Chromosoma* **106**, 348-60.

17. Martin, R. M., Gorisch, S. M., Leonhardt, H. & Cardoso, M. C. (2007). An Unexpected Link Between Energy Metabolism, Calcium, Chromatin Condensation and Cell Cycle. *Cell Cycle* **6**.

18. Cheutin, T., McNairn, A. J., Jenuwein, T., Gilbert, D. M., Singh, P. B. & Misteli, T. (2003). Maintenance of stable heterochromatin domains by dynamic HP1 binding. *Science* **299**, 721-5.

19. Schmiedeberg, L., Weisshart, K., Diekmann, S., Meyer Zu Hoerste, G. & Hemmerich, P. (2004). High- and low-mobility populations of HP1 in heterochromatin of mammalian cells. *Mol Biol Cell* **15**, 2819-33.

20. Manders, E. M., Verbeek, E. J. & Aren, J. A. (1993). Measurement of colocalization of objects in dual-colour confocal images. *J Microsc* **169**, 175-182.

21. Görisch, S. M., Richter, K., Scheuermann, M. O., Herrmann, H. & Lichter, P. (2003). Diffusion-limited compartmentalization of mammalian cell nuclei assessed by microinjected macromolecules. *Exp Cell Res* **289**, 282-94.

22. Dialynas, G. K., Terjung, S., Brown, J. P., Aucott, R. L., Baron-Luhr, B., Singh, P. B. & Georgatos, S. D. (2007). Plasticity of HP1 proteins in mammalian cells. *J Cell Sci* **120**, 3415-24.

23. Kanda, T., Sullivan, K. F. & Wahl, G. M. (1998). Histone-GFP fusion protein enables sensitive analysis of chromosome dynamics in living mammalian cells. *Curr Biol* **8**, 377-385.

24. Ellenberg, J., Lippincott-Schwartz, J. & Presley, J. F. (1999). Dual-colour imaging with GFP variants. *Trends Cell Biol* **9**, 52-6.

25. Campbell, R. E., Tour, O., Palmer, A. E., Steinbach, P. A., Baird, G. S., Zacharias, D. A. & Tsien, R. Y. (2002). A monomeric red fluorescent protein. *Proc Natl Acad Sci U S A* **99**, 7877-82.

26. Patterson, G. H. & Lippincott-Schwartz, J. (2002). A Photoactivatable GFP for Selective Photolabeling of Proteins and Cells. *Science* **297**, 1873-1877.

27. Cardoso, M. C., Joseph, C., Rahn, H. P., Reusch, R., Nadal-Ginard, B. & Leonhardt, H. (1997). Mapping and use of a sequence that targets DNA ligase I to sites of DNA replication in vivo. *J Cell Biol* **139**, 579-87.

28. Easwaran, H. P., Schermelleh, L., Leonhardt, H. & Cardoso, M. C. (2004). Replication-independent chromatin loading of Dnmt1 during G2 and M phases. *EMBO Rep* **5**, 1181-6.

29. Leonhardt, H., Rahn, H. P., Weinzierl, P., Sporbert, A., Cremer, T., Zink, D. & Cardoso, M. C. (2000). Dynamics of DNA replication factories in living cells. *J Cell Biol* **149**, 271-80.

30. Easwaran, H. P., Leonhardt, H. & Cardoso, M. C. (2007). Distribution of DNA replication proteins in Drosophila cells. *BMC Cell Biol* **8**, 42.

Figure legends

Fig 1 Manipulation and quantification of chromatin condensation states

Individual HeLa cells expressing H2B-GFP as a marker for chromatin[23] were visualized starting in mitosis (left panel) into G1 (mid panel) and following incubation in hyperosmolar medium (right panel). The cells were grown in DMEM with 10% fetal calf serum, 5 mM L-glutamine, 5 g/ml Gentamycine and the hypercondensation medium was composed of a dilution of 10x PBS in growth medium to yield 4x PBS equivalent to a 500 mM saline solution. Cells were in plated in 8-well Ibidi chambers (Ibidi, Munich, Germany). Live cell microscopy was performed with a Zeiss LSM510Meta confocal setup on a Zeiss Axiovert 200M inverted microscope with a 63x phase contrast plan-apochromat oil objective NA 1.4 (Carl Zeiss, Germany). The microscope is housed in a humidified chamber heated to 37°C (Okolab, Ottaviano, Italy). For acquisition the main beam splitter was HFT UV/488/543/633, GFP was excited by 488 nm Argon laser and detected with a 500-530 nm bandpass filter. Acquisition settings were identical for individual cells in repeated imaging experiments. At each time-point complete high resolution confocal z-stacks were acquired and projections are shown. Scale bar 5 µm. Chromatin volume calculations were derived from complete z-stacks and processed in Image J. Images were gauss filtered and background subtracted, then thresholded and the volumes calculated with the voxel counter plugin. The bar diagram summarizes the chromatin volume data as mean +/- standard deviation (N = ten cells) relative to the value for G1 interphase chromatin in the same cell.

Fig 2 Different pathways of chromatin condensation in mitosis and hyperosmolar condensation

A) Histone H3 is modified by phosphorylation at serine 10 during mitosis and was detected in formaldehyde fixed HeLa H2B-GFP cells using anti-phospho H3S10 specific antibodies. For immunofluorescence staining, cells were washed in PBS and, in case of hyperosmolar treatment incubated for 15 min in 4x PBS, fixed in 3.7% formaldehyde diluted in PBS or 4x PBS respectively and permeabilized with 0.25% Triton X100 in PBS. The primary anti-phospho H3 rabbit polyclonal antibody (catalog number 06-570, Millipore, Schwalbach, Germany) was diluted in PBS containing 0.2 % fish skin gelatin and detected using goat anti-rabbit IgG (Jackson, Newmarket, UK). In the

top panel the phosphorylated histone H3 signal (red) co-localizes with the histone H2B-GFP labeled chromosomes in the mitotic cell but it is not detected in the interphase cell. In the lower panel the chromatin was condensed by hyperosmolar treatment to induce a interphase chromatin volume comparable to mitotic chromosomes (see Fig 1). As in the untreated cells, the mitosis specific histone H3 phosphorylation is not detectable in the interphase nucleus and only in the mitotic chromosomes suggesting a different pathway of mitotic and hyperosmolar chromatin condensation.

The graph in B) displays intranuclear calcium levels in HeLa cells (N = 10) measured by timelapse microscopy using the fluorescent calcium sensor Fluo 3. The Fluo 3 (Invitrogen, Paisley, UK) labeling and measurements were performed as described before.[17] For untreated cells the initial Fluo 3 fluorescence intensity was normalized to 1 and, following the incubation in hyperosmolar 4x PBS solution, increased seven fold. To test for saturation effects and dynamic range of the Fluo 3 measurement conditions, the calcium ionophore ionomycin was added subsequently to the cells to induce maximum calcium uptake. This displays the whole range of fluorescence intensities measurable by the calcium sensor under the same imaging conditions and further suggests that the change in chromatin condensation after 4xPBS incubation involves a significant change in the calcium level. Scale bar 5 μm.

Fig 3 Distribution and mobility of chromatin proteins in different chromatin condensation states

HeLa cells stably expressing H2B-GFP as well as HeLa cells transiently transfected with plasmids coding for H2B-mRFP and either GFP-HP1α or PAGFP-HP1α were used in photobleaching or photoactivation experiments of the respective chromatin proteins as indicated.

The histone H2B-mRFP plasmid was constructed by cutting out CFP from pH2B-CFP[24] with BamHI + MfeI and ligating in the mRFP cDNA cut with EcoRI + BamHI from pRSET-mRFP1.[25] The photoactivatable HP1α construct was created by inserting the human HP1α cDNA derived from pBCHGN-HP1-alpha[18] cut with Hind III and BamH I into the Hind III and Bgl II of pPAGFP-C1.[26] Double transfection of cells was carried out by CaPO4 precipitation method[27] or using Transfectin reagent (BioRad, Munich, Germany). Live cell microscopy was performed as described

in Fig 1 and mRFP was excited by a 543 nm HeNe laser and detected using a 585-615 bandpass filter. Photobleaching and photoactivation were performed with a short intense pulse of 488 nm Argon laser beam. For all experiments, the areas photobleached (ba) and photoactivated (pa) are indicated by squares and the times after photobleaching/activation are given in the images. FRAP data were corrected for cell translational and rotational movements with the Image J 'stack_reg' plugin. The datasets were analyzed, evaluated and displayed in Origin 7. The photobleaching and photoactivation redistribution data were normalized, averaged and corrected for photobleaching or photoactivation by the image acquisition process. The half equilibrium times $t_{1/2}$ were derived in Origin 7 from bi-exponential decay fit curves.

The photobleaching experiment in A) shows histone H2B-GFP dynamics in interphase HeLa cells. Untreated interphase chromatin (top) and hyperosmolar condensed chromatin (bottom) are shown. In B) photobleaching experiments with HP1α-GFP are displayed for cells in interphase (top) and with hyperosmolar condensed interphase chromatin (bottom). Corresponding fluorescence recovery curves are shown on the right as the mean of ten cells with standard deviation. C) depicts the photoactivation experiments with HP1α fused to PAGFP. In the images before fluorescence activation the nucleus and chromosomes visualized independently with H2B-mRFP fusion are encircled by a dotted line. The dissociation of HP1α from chromatin measured by the loss of photoactivated fusion protein from the interphase chromatin is shown in the graphs on the right (mean of 10 cells with standard deviation). The insets in B) and C) are magnifications of the accumulations of HP1α at heterochromatin marked by the arrows.

Scale bars 5 µm.

Fig 4 Effect of chromatin condensation state on protein accessibility

The distribution of the inert tracer protein GFP, from the plasmid construct EGFP (Clontech, Heidelberg, Germany), and histone H2B-mRFP labeled chromatin is shown in representative optical sections of cells in mitosis (left column), in interphase (middle column) and in the same interphase cells again after induced chromatin condensation (right column). The double transfections and live cell microscopy were carried out as described in Fig 3 with identical acquisition settings for individual cells in repeated imaging experiments. Image analysis was performed with the Zeiss LSM Image Examiner software for fluorescence intensity and

colocalization measurements. The latter included the Pearson correlation coefficient (R), measured by selecting the nuclear areas excluding the nucleoli or for mitotic cells an oval area including the chromosomes and cytoplasm. The linescan analysis in B) displays the pixel intensity distribution of GFP (green) and chromatin (red) along the yellow arrow in the respective merged image in A). Regions with reduced protein concentration correspond to heterochromatin (arrow) and nucleoli (arrowhead). In C) the scatter plots display the pixel of the merged image according to the intensity values of the red and green channel and the frequency of the red-green pixel combination is coded by the color (hot colors represent higher frequencies). The red line demarcates the pixels corresponding to the mitotic chromosomes as well as to the interphase nucleus excluding the nucleoli (referred to as nucleoplasm). The Pearson correlation coefficient (R) is the mean ± standard deviation of 10 midsections in individual cells. Scale bar 5 µm.

Figure 1

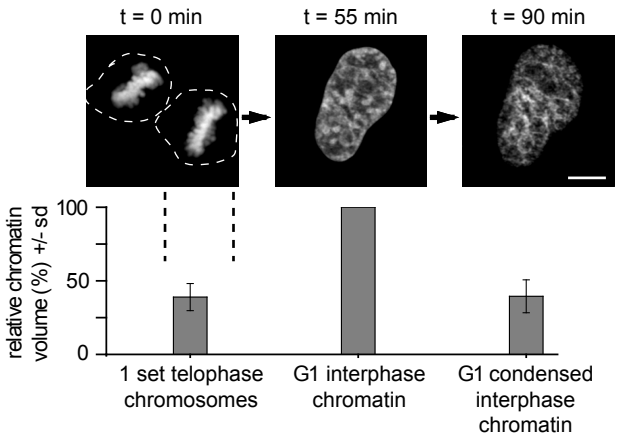
t = 0 min
t = 55 min
t = 90 min
relative chromatin volume (%) +/- sd
100
50
0
1 set telophase chromosomes
G1 interphase chromatin
G1 condensed interphase chromatin

Figure 2

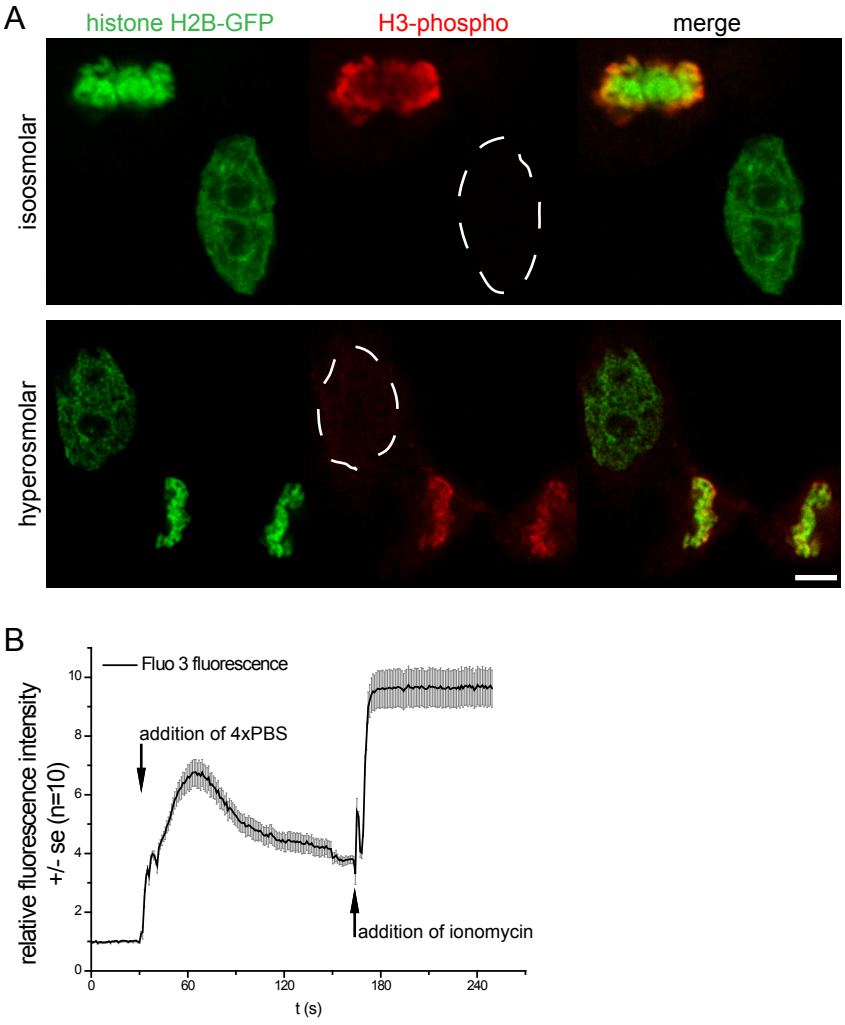
A
histone H2B-GFP
H3-phospho
merge
isoosmolar
hyperosmolar
B
Fluo 3 fluorescence
addition of 4xPBS
addition of ionomycin
relative fluorescence intensity
+/- se (n=10)
t (s)
0
2
4
6
8
10
0
60
120
180
240

Figure 3

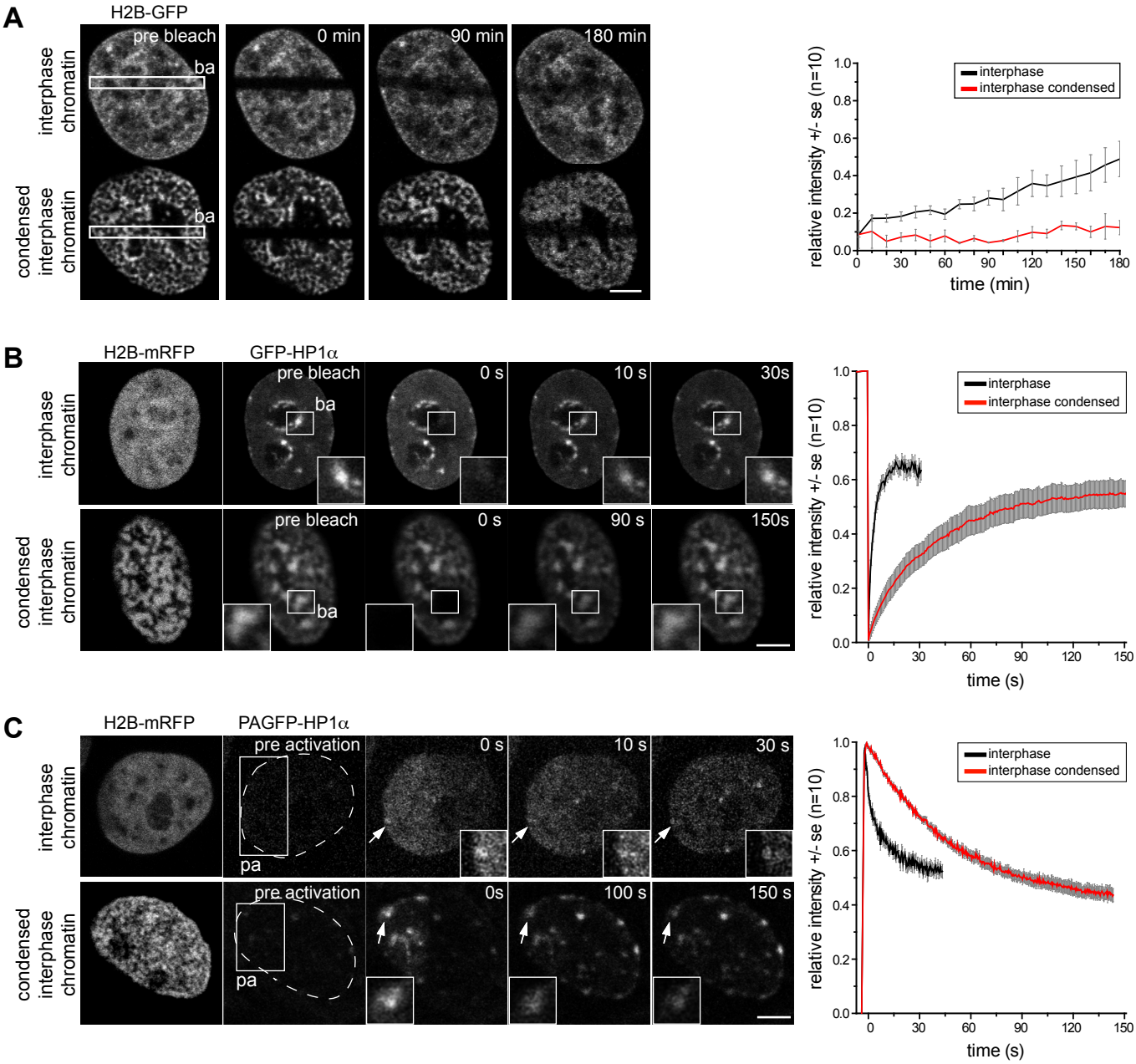
A
H2B-GFP
pre bleach
0 min
90 min
180 min
ba
interphase chromatin
condensed interphase chromatin
relative intensity +/- se (n=10)
interphase
interphase condensed
time (min)
B
H2B-mRFP
GFP-HP1α
pre bleach
0 s
10 s
30s
150s
90 s
time (s)
C
PAGFP-HP1α
pre activation
pa
0s
100 s
30 s

Figure 4

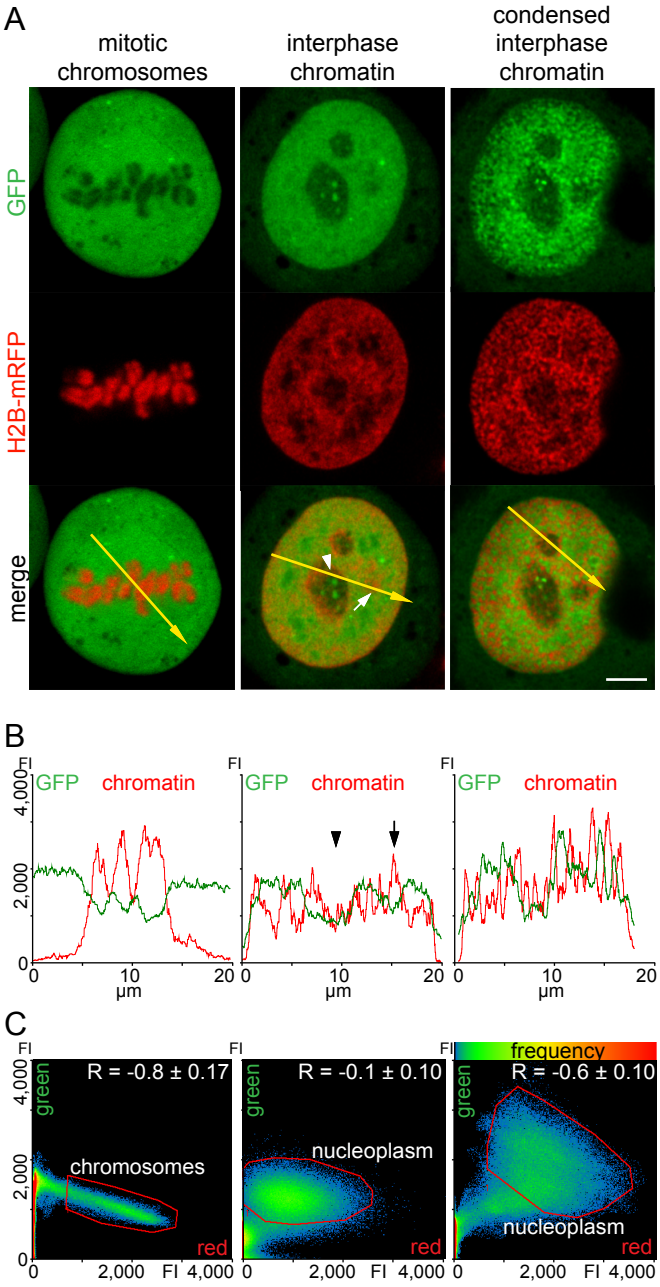
A
mitotic chromosomes
interphase chromatin
condensed interphase chromatin
GFP
H2B-mRFP
merge
B
FI
GFP
chromatin
4,000
2,000
0
10
20
µm
C
green
red
frequency
R = -0.8 ± 0.17
R = -0.1 ± 0.10
R = -0.6 ± 0.10
chromosomes
nucleoplasm
nucleoplasm
2,000
4,000

Figure S1

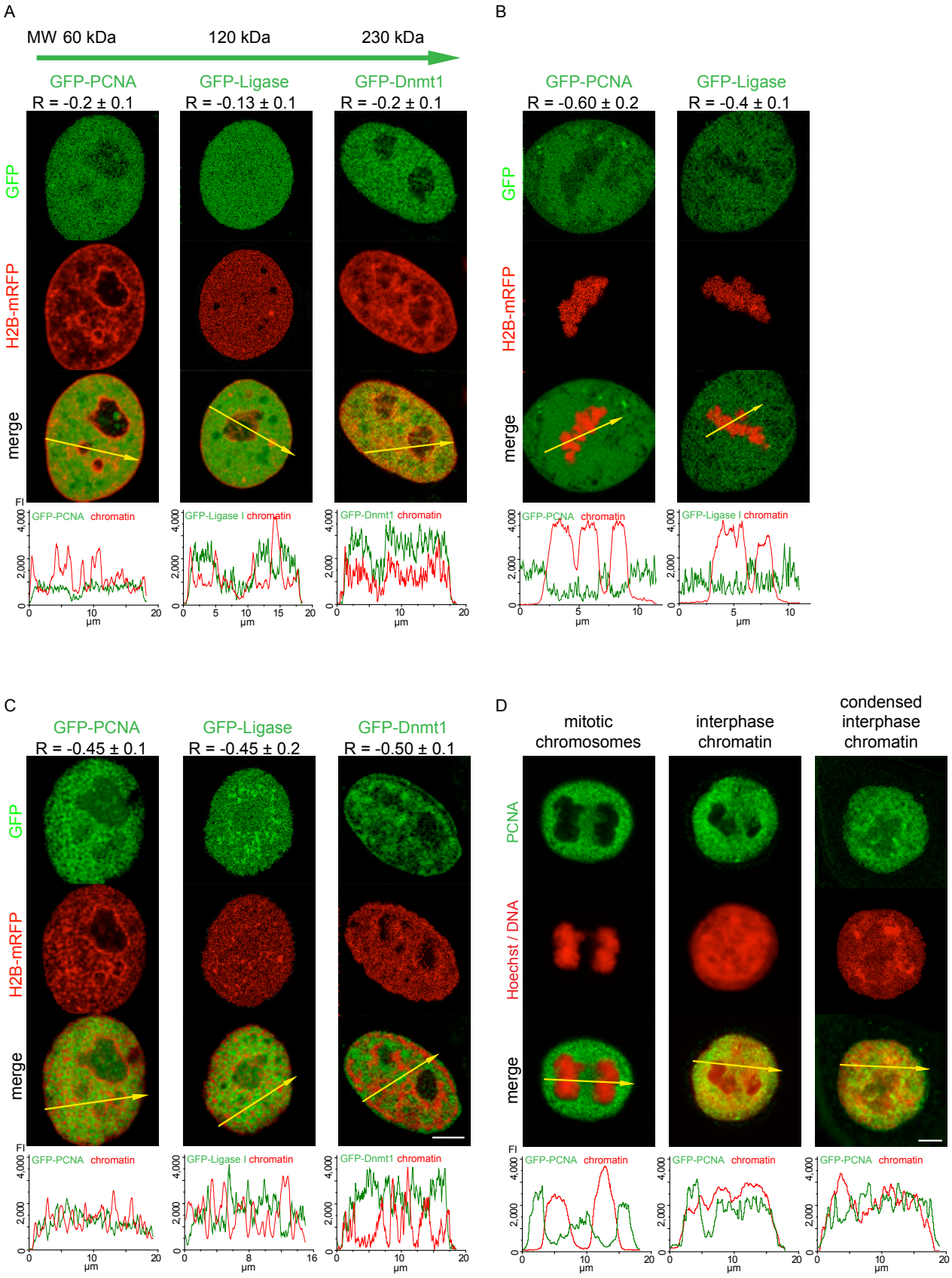
A
MW 60 kDa
120 kDa
230 kDa
GFP-PCNA
R = -0.2 ± 0.1
GFP-Ligase
R = -0.13 ± 0.1
GFP-Dnmt1
R = -0.2 ± 0.1
GFP
H2B-mRFP
merge
FI
GFP-PCNA chromatin
GFP-Ligase I chromatin
GFP-Dnmt1 chromatin
µm
B
GFP-PCNA
R = -0.60 ± 0.2
GFP-Ligase
R = -0.4 ± 0.1
C
GFP-PCNA
R = -0.45 ± 0.1
GFP-Ligase
R = -0.45 ± 0.2
GFP-Dnmt1
R = -0.50 ± 0.1
D
mitotic chromosomes
interphase chromatin
condensed interphase chromatin
PCNA
Hoechst / DNA

Fig S1 Effect of chromatin condensation state on accessibility of nucleoplasmic proteins of different size

Distribution of fusion proteins of different size GFP-DNA Ligase I, [27] GFP-Dnmt1 [28] and GFP-PCNA [29] in representative optical sections of live HeLa cells relative to chromatin labeled with H2B-mRFP in interphase A), mitosis B) and in C) the same cells as in A) upon hyperosmolar treatment yielding hypercondensation of chromatin to the level of mitotic chromosomes. The Pearson's correlation coefficients (R) given above the images were calculated excluding the nucleoli (mean of ten cells). The linescans below the images show the pixel intensity distribution along the direction of the arrow in the merged images.

In A) as with GFP alone the proteins were homogeneously distributed in the nucleoplasm as described before.[27,28,29] The lowest level of the fusion proteins was found in nucleoli and a slight reduction could be measured in large heterochromatin regions as displayed in the images and linescans. The increasing size of the proteins had no influence on their chromatin access in interphase nuclei as demonstrated by the correlation analysis (nucleoli excluded) with R-values between -0.13 and -0.2 indicating almost no correlation.

In B) cells in mitosis are shown with the chromosomes mostly excluding the proteins, supported by the drop of the protein fluorescence intensity in the area locating the condensed chromosomes in the linescans. The strong negative correlation coefficient with R-values of -0.6 and -0.4, respectively, further confirms the exclusion of non chromatin nuclear proteins from chromosomes. The GFP-Dnmt1 was not included in the mitosis analysis since it associates with constitutive heterochromatin from late S-phase to early G1.[28]

The hypercondensation of interphase chromatin in C) again leads to an exclusion of the fusion proteins from the condensed chromatin structures and an accumulation in the enlarged interchromatin space, This is also visible in the linescans by the inverse correlation of the protein and chromatin labeling intensity curves. Importantly, for interphase nuclei with induced hypercondensation of chromatin the Pearson coefficient for GFP fusion proteins drops to a level similar to mitotic cells R= -0.45 and -0.5 respectively.

In D) optical sections of fixed HeLa cells stained with an antibody to PCNA in mitosis, interphase and with interphase chromatin condensed to the mitotic chromosome volume are shown. Immunofluorescence staining was performed as described earlier.[30] As with the GFP fusions, in mitosis no protein labeling was visible in the chromosome area labeled with the DNA dye Hoechst 33258 whereas in interphase PCNA was distributed in the whole nucleus with some reduction in the nucleoli. Upon hyperosmolar condensation of interphase chromatin redistribution of the proteins could be observed with a concentration of protein in the enlarged interchromatin regions.

Scale bars 5 µm.